Chinese Chemical Letters 33 (2022) 5088–5091

Contents lists available at ScienceDirect

Chinese Chemical Letters

journal homepage: www.elsevier.com/locate/cclet

Atropisomer-based construction of a new perylene diimide macrocycle as visible-light photocatalyst for selective sulfide oxidation

Fei Yang[a], Miaomiao Zhen[a], Shanshan Wang[a,c], Wei Wei[b,*], Huan He[a], Yanqing Xu[a,*]

[a] Key Laboratory of Cluster Science, Ministry of Education of China, Beijing Key Laboratory of Photoelectronic/Electrophotonic Conversion Materials, School of Chemistry and Chemical Engineering, Beijing Institute of Technology, Beijing 100081, China
[b] Department of Chemistry, Capital Normal University, Beijing 100048, China
[c] Test & Analysis Center of Shougang Technical Research Institute, Beijing 100043, China

ARTICLE INFO

Article history:
Received 30 December 2021
Revised 29 March 2022
Accepted 31 March 2022
Available online 6 April 2022

Keywords:
Macrocycles
Perylene diimine
Photocatalysis
Atropisomer
Selective oxidation

ABSTRACT

By using a perylene diimine (PDI) *syn*-atropisomer as highly preorganized precursor, we successfully constructed a visible-light-active organic macrocycle **PDI-M**. The formation of macrocyclic structure effectively avoids self-aggregation of PDI cores and enhances the absorption in visible region. As a photocatalyst, **PDI-M** exhibits excellent activity on aerobic selective oxidation of sulfide into sulfoxide under visible light irradiation at room temperature. Mechanism studies show that both superoxide and singlet oxygen act as reactive oxygen species. This work provides a typical case toward the maximum utilization of photosensitive groups under mild conditions.

The preparation of artificial organic macrocycles, especially those with functional groups, has always been a hot spot in the field of supramolecular chemistry [1,2]. The yield of ring-closing reaction is relatively low, due to the formation of polymeric by-products. To overcome the difficulties caused by the traditional method of high dilution and template synthesis, we recently have proposed a strategy of using a naphthalimide atropisomer as a highly preorganized precursor to prepare organic macrocycles (Scheme 1). The macrocycles were obtained in an excellent ring-closing yield reaching ~90% and exhibited a selective recognition for tryptophan [3]. As an important extension of this efficient strategy, we wished to explore the preparation of perylene diimide-based (PDI) macrocycles with larger conjugated structure as molecular skeleton. It is well known that PDI and its derivatives are a class of dye molecules with excellent photoelectrical properties. Due to their cheap source, high electron mobility, strong absorption capacity and adjustable electronic energy levels by chemical modification, they have shown a wide range of potential applications in many fields such as organic solar cells [4–6], organic field effect transistors [7–9], fluorescent probe sensing materials [10–13], photodynamic and photothermal therapy in biomedical [14–16]. Thus, to use PDI as the building blocks may bring abundant photoelectrical functions to the organic macrocycles. But so far, due to low solubility and other reasons, PDI-based macrocycles are still relatively limited [17–19] and further exploration is urgently needed.

Photocatalysis is an important branch of catalysis, which can convert solar energy into chemical or electrical energy to initiate organic reaction *via* thermal activation process. Compared with ultraviolet radiation, the visible-light driven photocatalysis is more attractive and has developed into a mild, clean and atomic efficient organic synthesis method [20–24]. PDI derivatives as excellent visible-light absorbing materials, however, tend to self-aggregate together due to their rigid large π-conjugated planar structures, resulting in fluorescence quenching and greatly reducing the utilization efficiency of photosensitive groups [25]. So far, there are still relatively limited investigations on the PDI photocatalysts driven by visible light [26–29].

Encouraged by the high efficiency of our macrocyclization strategy [3], we herein prepared a PDI-based *syn*-atropisomer as highly preorganized precursor to successfully construct a new visible-light-active organic macrocycle **PDI-M**. The formation of macrocyclic structure effectively avoids self-aggregation of PDI cores and enhances the absorption in the visible region. As an efficient photocatalyst, **PDI-M** can catalyze oxidation reaction of a series of thioethers into corresponding sulfoxides in a high conversion and selectivity both exceeding 90%. The reaction proceeded smoothly under mild conditions utilizing visible light as the driving force and molecular oxygen as the oxidant at room temperature.

* Corresponding authors.
E-mail addresses: wwei@cnu.edu.cn (W. Wei), xyq@bit.edu.cn (Y. Xu).

https://doi.org/10.1016/j.cclet.2022.03.123
1001-8417/

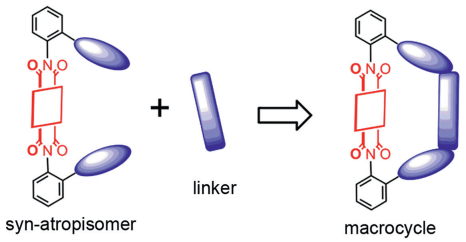

Scheme 1. The synthetic strategy of macrocycle based on arylenediimide *syn*-atropisomers.

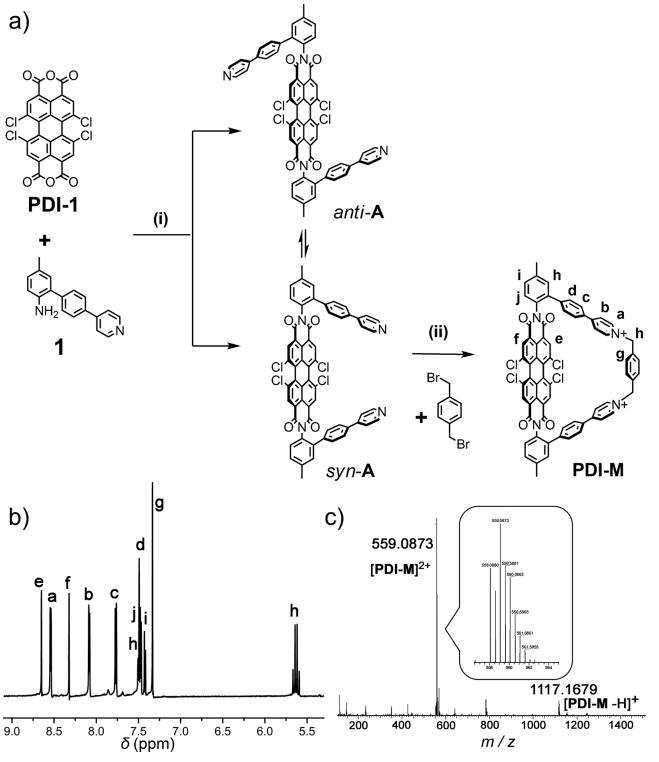

Fig. 1. (a) Synthesis of **PDI-M**: (i) CH_3CH_2COOH, 145 °C, 10 h; (ii) CH_3CN/CH_2Cl_2, 70 °C, 18 h. (b) ^1H NMR spectrum (DMSO-d_6, 298 K) and (c) high resolution ESI-MS of **PDI-M**·$2PF_6$.

The synthesis of macrocycle **PDI-M** is illustrated in Fig. 1. Firstly, arylamine **1** was obtained by a Suzuki coupling reaction between corresponding aryl bromide and boronic acid (Figs. S1-S4 in Supporting information). Then, an imide condensation of the as-prepared **1** with 1,6,7,12-tetrachloro-3,4,9,10-perylene tetracarboxylic dianhydride (**PDI-1**, Fig. S1) in propionic acid to form a mixture of *syn*- and *anti*-PDI atropisomers (*syn*-**A** and *anti*-**A**, respectively). Owing to the difference in polarity, the *syn*-/*anti*-arylenediimide atropisomers were usually separated by column chromatography in the previous work [3,30-33]. Interestingly, the isomers in this work can be directly separated by solubility difference and no column separation is required. As shown in Figs. S5-S7 (Supporting information), the purity of the products is proved. That is, only precursor *syn*-**A** with convergent conformation precipitated after the reaction, and pure *syn*-**A** can be obtained by simple filtration and washing. This extraordinary discrepancy in solubility is probably derived from the extended length of pendant 4-pyridylphenyl groups, which lead to larger polarity difference between *syn*- and *anti*-isomers. With quantities of precursor *syn*-**A** in hand, macrocycle **PDI-M** as dibromide salt was synthesized in a straightforward manner after reacting with linker 1,4-bis(bromomethyl)benzene in acetonitrile/chloroform for 18 h at 70 °C. The whole cyclization reaction did not need operationally complex conditions such as the use of highly diluted concentration, template molecules and slow dropwise addition of reactants. The product as chloride (**PDI-M**·2Cl) and PF_6 salt (**PDI-M**·$2PF_6$) can be obtained by anion exchange. ^1H NMR spectrum of **PDI-M** indicated the existence of a single symmetrical structure (Fig. 1b) and high resolution electrospray-ionization mass spectrometry (ESI-MS) analysis also showed peaks of **PDI-M** with the loss of two counterions (Fig. 1c).

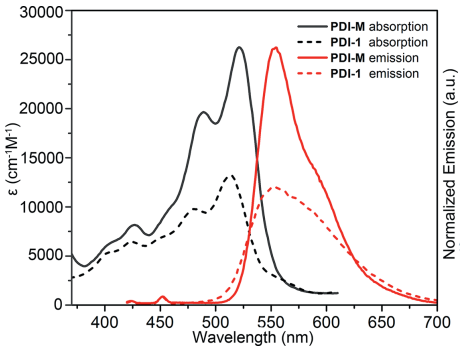

Fig. 2. Absorption and emission spectra of **PDI-M** (solid line) and 1,6,7,12-tetrachloro-3,4,9,10-perylenetetracarboxylic dianhydride (**PDI-1**, dashed line) in DMF (0.01 mmol/L).

As shown by Fig. 2, the UV-vis absorption and fluorescence emission spectra of **PDI-M** and reactant **PDI-1** were investigated. The macrocycle **PDI-M** shows strong absorption in the range of 400-550 nm and fluorescence emission centered at 560 nm, which are significantly enhanced compared with that of **PDI-1**. These results are probably due to the macrocyclic structure of **PDI-M** that prevents the aggregation of chromophores and enhances their solubility. Cyclic voltammogram showed that the potentials of the two reversible single electron reduction waves are −0.39 and −0.84 eV *vs.* Ag/AgCl (Fig. S13 in Supporting information). We used the Rehm-Weller formula to calculate the Gibbs free energy (Table S1 in Supporting information), which are attributed to the formation of charge-delocalized radical anion $PDI^{\cdot-}$ and the dianion PDI^{2-} of the macrocyclic compound **PDI-M**.

The catalytic performance of **PDI-M**·2Cl was evaluated in the selective oxidation of thioanisole under visible light (λ = 455 nm blue LED) and oxygen atmosphere at room temperature (Table 1). The reaction was firstly performed in acetonitrile, but only 10% of sulfide was converted with a low sulfoxide selectivity (25%). Solvent optimization showed that the mixed solvent of CH_3CN and water is favorable to the selective oxidation of sulfide to sulfoxide (entries 1-7). The optimal ratio of CH_3CN/H_2O is approximately 7:2, which can significantly improve the conversion and selectivity up to 96% and 92% (entry 7). An excess of photocatalyst was demonstrated to lead to a decrease in yield (Table S2 in Supporting information). For the existence of the arm charges and the closed ring, the catalyst is found slightly soluble in water and redundant powders were found to suspend on the surface of reaction system, which probably reduces the absorption of light energy. The time profile for sulfide oxidation showed that high conversion and selectivity was simultaneously obtained in *ca.* 2 h (Fig. S14 in Supporting information). Upon prolonged reaction, the conversion can reach nearly 100%, while the selectivity of sulfoxide decreased slightly because of overoxidation. To show the practicability of this method, a gram-scale reaction was carried out, producing the desired product sulfoxide in 87% yield (1.218 g). The control experiments indicated that no reaction occurred in the absence of light (entry 9), photocatalyst (entry 10) or O_2 (entry 11).

Table 1
Optimization of photocatalytic oxidation conditions of thioanisole.

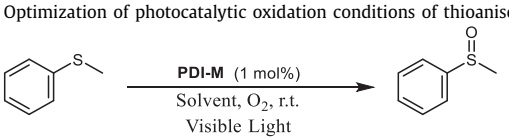

Entry	Solvent	Catalyst	Conversion (%)	Sulfoxide selectivity (%)
1	CH_3CN	**PDI-M**	10	25
2	CH_2Cl_2	**PDI-M**	11	62
3	CH_3CH_2OH	**PDI-M**	41	78
4	CH_3OH	**PDI-M**	47	80
5	H_2O	**PDI-M**	70	4
6[a]	CH_3CN+H_2O	**PDI-M**	95	88
7[b]	CH_3CN+H_2O	**PDI-M**	96	92
8[c]	CH_3CN+H_2O	**PDI-M**	52	80
9[d]	CH_3CN+H_2O	**PDI-M**	Trace	Trace
10	CH_3CN+H_2O	-	Trace	Trace
11[e]	CH_3CN+H_2O	**PDI-M**	Trace	Trace
12[b]	CH_3CN+H_2O	**PDI-1**	20	72
13[b]	CH_3CN+H_2O	**PDI-2**	5	55
14[b]	CH_3CN+H_2O	**PDI-3**	93	91

All reactions were carried out on a scale of 0.45 mmol thioanisole, 1% mol catalyst and 0.36 mmol biphenyl in 4.5 mL of solvent under visible light at room temperature for 2 h, equipped with an oxygen balloon.
[a] $CH_3CN/H_2O=8/1$.
[b] $CH_3CN/H_2O=7/2$.
[c] $CH_3CN/H_2O=2/1$.
[d] Without light.
[e] Under a nitrogen atmosphere. **PDI-1**, **PDI-2 and PDI-3** (Table S3 in Supporting information). Conversion and selectivity calculated from GC.

With the optimal reaction conditions, the compared catalytic activities of acyclic monomers **PDI-1** and **PDI-2** were carried out. They exhibited poor conversion rate and selectivity (entries 12 and 13), which may be ascribed to both the poor solubility and the aggregation of the PDI photosensitizers. To further confirm this assumption, a charged monomeric **PDI-3** instead of neutral **PDI-1**/**PDI-2** was designed and synthesized (Fig. S1). This parallel experiment was labeled as entry 14. As anticipated, a satisfied catalytic effect as **PDI-M** was obtained for its full solubility and non-aggregation from two extended charged arms. It is worth noting that the solubility of **PDI-M** in CH_3CN/H_2O (7:2) is only approximately 1% of **PDI-3** (Table S3), so a much less amount of **PDI-M** catalyst would achieve the comparable catalytic effect as that of **PDI-3**. From the above-mentioned experiments, we can summarize that there are two advantages in our titled macrocycle: i) the macrocyclic structure prevents the aggregation of PDI mother nucleus; ii) the attached charged groups make an observable dissolution in a minor amount of H_2O, and thus only a very small amount of catalyst is needed.

The excellent activity and selectivity of **PDI-M** for the transformation of thioanisole to sulfoxide prompted us to explore other thioethers as substrate under the optimal reaction conditions. Considering the electronic effects of different substituent groups on the phenyl groups, a series of substrates with the various election withdrawing or donating groups are chosen as displayed in Table 2. Though the *para*-substitution with electron withdrawing groups on the benzene ring seems slightly suppresses the sulfide oxidation to a degree than the donating groups, the experimental results exhibited good photocatalytic activity of **PDI-M** for all the tested substrates from aryl to alkyl thioether, which give us an overall impression that the title macrocycle could function as universal catalyst for the oxidation of thioether to sulfoxide.

To reveal the mechanism of the photooxidative reaction, additional experiments were performed. Radical scavengers including quinol for radicals, *p*-benzoquinone for $O_2^{\cdot-}$/$^{\cdot}OH$, *tert*-butyl alcohol for $^{\cdot}OH$ and DMPO for $O_2^{\cdot-}$ were used in the selective oxidation of sulfide (Table 3). We found that the photooxidative reaction

Table 2
Substrate expansion for photocatalytic oxidation by **PDI-M**.

Entry	Substrate	Time (h)	Conversion (%)	Sulfoxide Selectivity (%)
1		2	96	92
2	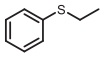	2	94	92
3	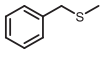	2	92	90
4	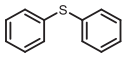	4	89	85
5	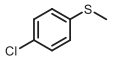	4	91	93
6	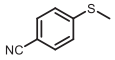	4	89	87
7	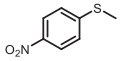	4	87	81
8	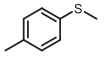	2	98	94
9	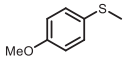	2	98	96
10		2	97	94
11	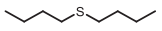	2	94	92

All reactions were conducted on a scale of 0.45 mmol sulfides, 1% mol **PDI-M** and 0.36 mmol biphenyl in 4.5 mL of mixed solvent ($CH_3CN/H_2O=7/2$) under visible light at room temperature, equipped with an oxygen balloon. Conversion and selectivity calculated from GC.

Table 3
Free radical scavenging experiments.

Entry	Radical scavengers	Scavenging group	Conversion (%)
1	-	-	96
2	Quinol	radicals	1
3	*p*-Benzoquinone	$O_2^{\cdot-}$ / $^{\cdot}OH$	9
4	*tert*-Butyl alcohol	$^{\cdot}OH$	87
5	DMPO	$O_2^{\cdot-}$	3
6	TEMP	$^1O_2$	28

Conversion and selectivity calculated from GC.

of sulfides can be significantly suppressed after adding quinol, *p*-benzoquinone and DMPO (entries 2, 3 and 5), whereas *tert*-butyl alcohol does not evidently change the reaction (entry 4), indicating that the reaction process involves $O_2^{\cdot-}$ radicals. Meanwhile, the conversion of sulfide was also inhibited after adding TEMP (entry 6), a singlet oxygen trap. Therefore, $O_2^{\cdot-}$ and $^1O_2$ species were simultaneously present in the reaction process. These observations are in accordance with the previously reported mechanism [26,34], that is, singlet oxygen oxidation through an energy transfer coexisting with a radical pathway through electron transfer.

Other experiments further supported the proposed mechanism. As shown by Table 1, when water was added to the acetonitrile re-

action system, the conversion rate and selectivity were greatly improved, so we wondered whether H_2O could act as reactant to be involved in the reaction process. To explore the origin of O in the product sulfoxide, an isotope labeling experiment was performed using H_2O^{18} and H_2O. No product of sulfoxide containing O^{18} was detected in the reaction system when using H_2O^{18} as solvent by GC-MS (Fig. S15 in Supporting information). Thus, it can be concluded that O_2 rather than H_2O acts as the only oxygen source to afford the product sulfoxide. According to the reported literature [35], the charged intermediates formed through $^1O_2$ oxidation can be effectively stabilized in the polar solvents containing protons, thereby accelerating the reaction rate, which implies the presence of singlet oxygen in the reaction. On the other hand, it is well known that $O_2^{\cdot-}$ is formed by the electron transfer between the triplet sensitizer and the oxygen molecule. We used the Rehm-Weller formula to calculate the Gibbs free energy for electron transfer between the photosensitizer and the substrate (Table S1) [36]. The Gibbs free energy of electron transfer from methyl phenyl sulfide to **PDI-M** excited state is −2.07 eV, and the value of **PDI-M** excited state to O_2 with the formation of $O_2^{\cdot-}$ is −1.64 eV. Taking the favorable Gibbs free energy into account in both of the electron-transfer steps, the generation of superoxide anion radical in the reaction is reasonable.

Based on the above mechanism experiments, we conclude that there may be two paths for the sulfide oxidation in this system (Fig. S16 in Supporting information): (i) Energy transfer path: after absorbing photons, the excited PDI* transfers energy through intermolecular transfer to O_2, forming $^1O_2$. The singlet oxygen can seize an electron of sulfide to form R_2S^+-OO^-, which further reacts with another sulfide molecule to afford the product sulfoxide. (ii) Single electron transfer path: one electron is first transferred from sulfide to the excited PDI* form the electron-losing thioether and $PDI^{\cdot-}$, and then $PDI^{\cdot-}$ transfers one single electron to O_2, forming $O_2^{\cdot-}$. Subsequently, the electron-losing thioether is oxidized by $O_2^{\cdot-}$ to generate sulfoxide.

In summary, a novel PDI-based macrocycle **PDI-M** was successfully designed and synthesized from a highly preorganized atropisomer precursor. As an efficient and environmental-friendly photocatalyst, **PDI-M** was employed for selective oxidation of sulfides to sulfoxides under visible light using O_2 as oxidant at room temperature. Taking the advantage in avoiding the aggregation of PDI cores into account, visible-light-active macrocycles may act as promising photocatalysts for organic reactions.

Declaration of competing interest

The authors declare that they have no known competing financial interests or personal relationships that could have appeared to influence the work reported in this paper.

Acknowledgments

This study was supported by the National Natural Science Foundation of China (No. 22171021), Yanjing Young Scholar Candidate Program of Capital Normal University, Capacity Building for Sci-Tech Innovation-Fundamental Scientific Research Funds.

Supplementary materials

Supplementary material associated with this article can be found, in the online version, at doi:10.1016/j.cclet.2022.03.123.

References

[1] K.D. Xu, Z.Y. Zhang, C.M. Yu, et al., Angew. Chem. Int. Ed. 59 (2020) 7214–7218.
[2] L.P. Yang, L.P. Yang, H. Yao, et al., Acc. Chem. Res. 53 (2020) 198–208.
[3] F. Yang, C. Liu, D. Yin, et al., Chem. Commun. 55 (2019) 14335–14338.
[4] Y. Lin, Y. Wang, J. Wang, et al., Adv. Mater. 26 (2014) 5224.
[5] K. Ding, Y. Wang, T. Shan, et al., Org. Electron. 78 (2020) 105569.
[6] K. Wang, P. Xia, K. Wang, et al., ACS Appl. Mater. Inter. 12 (2020) 9528–9536.
[7] S.R. Puniredd, A. Kiersnowski, G. Battagliarin, et al., J. Mater. Chem. C 1 (2013) 2433.
[8] M. Vespa, J.R. Cann, S.V. Dayneko, et al., Eur. J. Org. Chem. 2018 (2018) 4592–4599.
[9] J.D. Yuen, V.A. Pozdin, A.T. Young, et al., Dyes Pigments 174 (2020) 108014.
[10] X. Zhang, Y. Yan, Q. Peng, J. Wang, Y. Hang, J. Hua, Mater. Chem. Front. 1 (2017) 2292–2298.
[11] P. Singh, L.S. Mittal, H. Singh, et al., New. J. Chem. 41 (2017) 10281–10290.
[12] D. Sriramulu, S. Valiyaveettil, Dyes Pigments 134 (2016) 306–314.
[13] L. Yan, L. Yang, J. Lan, et al., Sci. China Chem. 52 (2009) 518–522.
[14] X. Hu, F. Lu, L. Chen, et al., ACS Appl. Mater. Inter. 9 (2017) 30458–30469.
[15] P. Sun, X. Wang, G. Wang, et al., J. Mater. Chem. B 6 (2018) 3395–3403.
[16] Q. Gong, J. Xing, Y. Huang, et al., ACS Appl. Bio. Mater. 3 (2020) 1607–1615.
[17] F. Würthner, C.R. Saha-Möller, B. Fimmel, et al., Chem. Rev. 116 (2016) 962–1052.
[18] M. Sapotta, Hofmann A, Bialas D, et al., Angew. Chem. Int. Ed. 58 (2019) 3516–3520.
[19] T.A. Barendt, L. Ferreira, I. Marques, et al., J. Am. Chem. Soc. 139 (2017) 9026–9037.
[20] D.M. Schultz, T.P. Yoon, Science 343 (2014) 985.
[21] L. Marzo, S.K. Pagire, O. Reiser, et al., Angew. Chem. Int. Ed. 57 (2018) 10034–10072.
[22] M.H. Muhammad, X.L. Chen, Y. Liu, et al., ACS Sustain. Chem. Eng. 8 (2020) 2682–2687.
[23] S. He, X. Chen, F. Zeng, et al., Chin. Chem. Lett. 31 (2020) 1863–1867.
[24] Y. Ma, F. Gao, W. Xiao, et al., Chin. Chem. Lett. 33 (2022) 4395–4399.
[25] G. Zhang, X. Xu, Y.W. Lee, et al., Adv. Funct. Mater. 29 (2019) 1902079.
[26] Y. Gao, H. Xu, S. Zhang, et al., Org. Biomol. Chem. 17 (2019) 7144–7149.
[27] L. Zeng, T. Liu, C. He, et al., J. Am. Chem. Soc. 138 (2016) 3958–3961.
[28] I. Ghosh, T. Ghosh, J.I. Bardagi, et al., Science 346 (2014) 725–728.
[29] C.J. Zeman, S. Kim, F. Zhang, et al., J. Am. Chem. Soc. 142 (2020) 2204–2207.
[30] K.D. Shimizu, T.M. Dewey, J.J. Rebek, J. Am. Chem. Soc. 116 (1994) 5145–5149.
[31] K. Kishikawa, C. Iwashima, S. Kohmoto, et al., J. Chem. Soc. Perkin Trans. 1 (2000) 2217–2221.
[32] Y.S. Chong, M.D. Smith, K.D. Shimizu, J. Am. Chem. Soc. 123 (2001) 7463–7464.
[33] Y. Zhao, N. Sakai, S. Matile, Nat. Commun. 5 (2014) 3911.
[34] L. Tang, K. Du, B. Yu, L. He, Chin. Chem. Lett. 31 (2020) 2991–2992.
[35] S.M. Bonesi, I. Manet, M. Freccero, et al., Chem. Eur. J. 12 (2006) 4844–4857.
[36] D. Rehm, A. Weller, Isr. J. Chem. 8 (1970) 259–271.